Chemical Science

ROYAL SOCIETY OF CHEMISTRY

EDGE ARTICLE

View Article Online
View Journal | View Issue

Cite this: *Chem. Sci.*, 2025, **16**, 5166

All publication charges for this article have been paid for by the Royal Society of Chemistry

Received 19th December 2024
Accepted 13th February 2025

DOI: 10.1039/d4sc08569h

rsc.li/chemical-science

Template-directed self-assembly of porphyrin nanorings through an imine condensation reaction†

Ziwei Xu,[a] Xinwen Ying,[a] Yi Li,[a] Xiaoyan Dong,[a] Jiyong Liu,[d] Shuping Wang,[a] Marc A. Little,[b] Dahao Zhang,[a] Yongshu Xie,[c] Zibin Zhang,[a] Ling Yu,[a] Feihe Huang[de] and Shijun Li*[a]

Template-directed self-assembly has proven to be an extremely effective method for the precise fabrication of biomacromolecules in natural systems, while artificial template-directed self-assembly systems for the preparation of highly intricate molecules remain a great challenge. In this article, we report the template-directed self-assembly of porphyrin nanorings with different cavity sizes from a tetraaldehyde-derived Zn(II) porphyrin and a diamine precursor through an imine condensation reaction. Up to 9 or 18 precursor molecules self-assemble together to produce a triporphyrin nanoring and a hexaporphyrin nanoring in one step, with the assistance of a tripyridine or hexapyridine template, respectively. The imine-linked porphyrin nanorings are further modified by reduction and acylation reactions to obtain more stable nanorings. The open cavities of porphyrin rings enable them to act as effective hosts to encapsulate fullerenes (C_{60} and C_{70}). This work presents a highly efficient template-directed self-assembly strategy for the construction of complicated molecules by using dynamic covalent chemistry of imine bond formation.

Introduction

Molecular design for the synthesis of complicated molecules with inherent structural beauty and fascinating functions is the persistent aspiration of chemists. Molecular cages[1] are a class of typical representatives. In the past two decades, molecular cages have attracted much more attention owing to their broad application prospects in guest encapsulation and controlled release,[2] chiral separation and catalysis,[3] nanoreactors,[4] gas absorption and separation,[5] and so on. Traditionally, there are two methods that can be used to prepare molecular cages: (1) self-assembly through noncovalent interactions; (2) formation through covalent bonds. The strength of a single noncovalent bond is far less than that of a covalent bond, so the molecular cages formed by noncovalent bonds are usually unstable and fragile.[6] Comparatively, molecular cages that are constructed by covalent bonds with large bond energies generally have good stability.[7] However, the formation of most covalent bonds is under kinetic control, which usually leads to low efficiency in the generation of molecular cages. To overcome this issue, dynamic covalent chemistry (DCC),[8] a kind of chemical method based on reversible covalent bond formation reactions, has been widely introduced for the preparation of molecular cages.[9] Among them, the reversible condensation of amines and aldehydes to form imine bonds is one of the most successful DCC reactions.[10] The formation of imine bonds is a reversible reaction with the ability to "self-correct" and "proofread", providing a valuable opportunity for the synthesis of stable target molecules under thermodynamic control.[11] Thanks to its dynamic reversibility and ease of formation, molecular cages based on imine structures are highly favoured by researchers.[12] Although covalent molecular cages based on imine bond formation have achieved great success, the design of cages with intriguing topological architecture and useful functions is still highly demanded.[13]

Additionally, it is of great significance to introduce functional groups into molecular cages for acquiring desired

[a]College of Material, Chemistry and Chemical Engineering, Key Laboratory of Organosilicon Chemistry and Material Technology of Ministry of Education Hangzhou Normal University, Hangzhou 311121, P. R. China. E-mail: l_shijun@hznu.edu.cn

[b]Department of Chemistry and Materials Innovation Factory, University of Liverpool, Liverpool L7 3NY, UK

[c]Key Laboratory for Advanced Materials and Institute of Fine Chemicals, School of Chemistry and Molecular Engineering, East China University of Science & Technology, Shanghai, 200237, P. R. China

[d]Stoddart Institute of Molecular Science, Department of Chemistry, Zhejiang University, Hangzhou 310027, P. R. China

[e]Zhejiang-Israel Joint Laboratory of Self-Assembling Functional Materials, ZJU-Hangzhou Global Scientific and Technological Innovation Center, Zhejiang University, Hangzhou 311215, P. R. China

† Electronic supplementary information (ESI) available: Synthesis and characterization of the porphyrin nanorings, detailed crystallographic data, host–guest complexation data and investigation on selective complexation of C_{60}/C_{70}. CCDC 2403445. For ESI and crystallographic data in CIF or other electronic format see DOI: https://doi.org/10.1039/d4sc08569h

functions and specific applications.[14] Introducing porphyrin units with excellent photophysical and redox properties into molecular cages endows them with important application values.[15] Use of porphyrin precursors is the most simple and convenient method to introduce porphyrin functional groups. Herein, we present a template-oriented self-assembly strategy[16] to synthesize multi-porphyrin imine nanorings starting from a tetra-substituted porphyrin monomer with aldehyde functional groups through a one-step imine bond formation reaction with a carefully selected diamine. Triporphyrin and hexaporphyrin nanorings were prepared by using a tripyridyl or hexapyridyl template,[17] respectively. The combined use of dynamic covalent imine bond formation and the template-directed strategy can make this method more efficient for the synthesis of porphyrin nanorings. Another advantage of this method is the use of more easily available tetra-substituted porphyrin monomers, but not *trans*-disubstituted porphyrin monomers that are usually synthesized using multiple steps and in lower yields. The prepared porphyrin nanorings have unique cylindrical three-dimensional cavities, which facilitate the encapsulation of fullerenes C_{60} and C_{70}. It was found that these porphyrin nanorings could form 1 : 1 host–guest complexes with the fullerene C_{60} or C_{70} and the triporphyrin nanoring could selectively encapsulate C_{70}, which is expected to be used for selective adsorption and separation of C_{70}.

Results and discussion

Synthesis of triporphyrin nanorings

The synthetic route of porphyrin nanorings is shown in Scheme 1. With 5,10,15,20-tetrakis(4-formylphenyl)porphyrin as the starting material, zinc acetate was employed to coordinate the

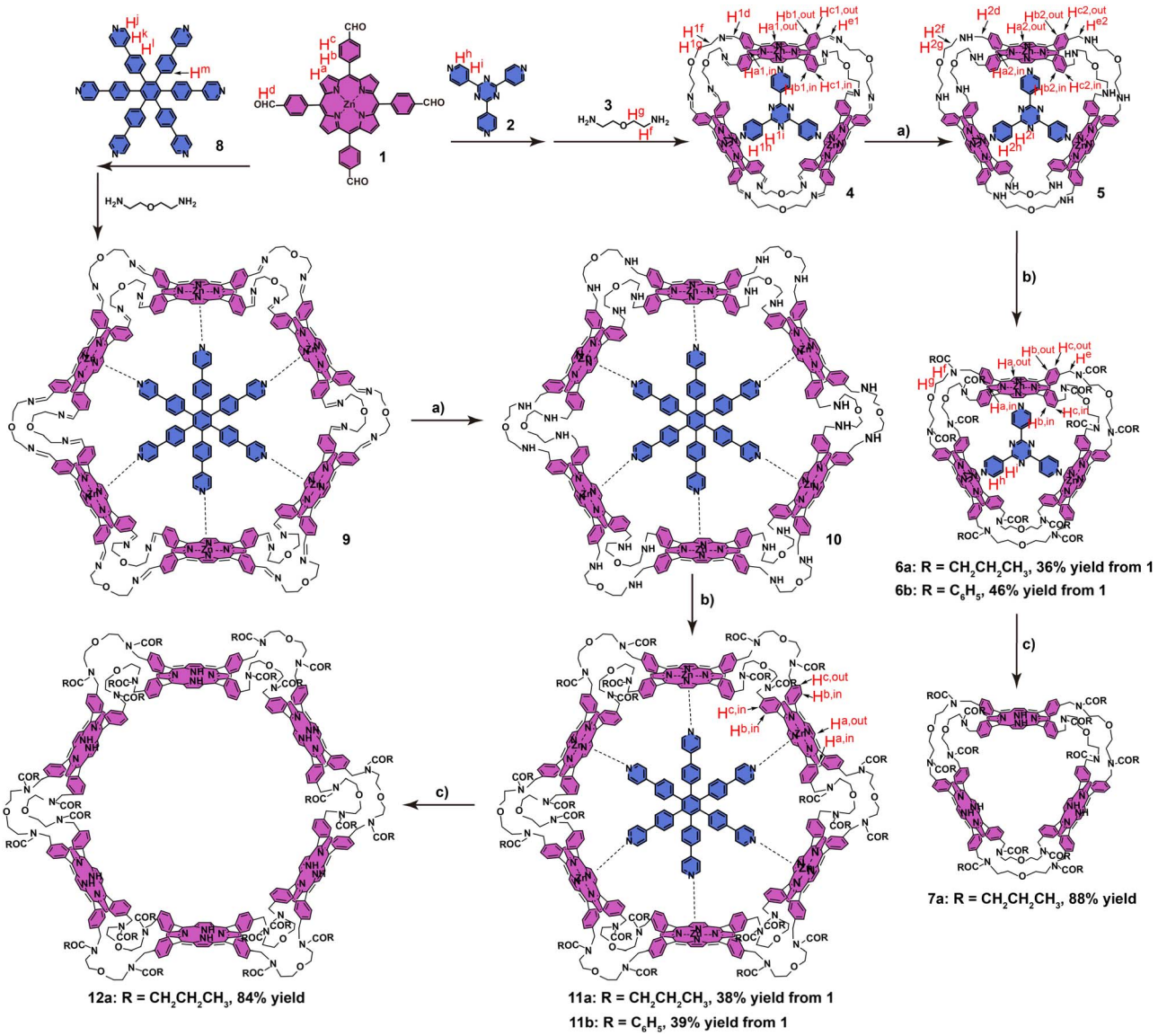

Scheme 1 Template-directed synthesis of triporphyrin nanorings and hexaporphyrin nanorings. [a]Reaction conditions: (a) $NaBH(CH_3COO)_3$, $CHCl_3$, r.t.; (b) $CH_3CH_2CH_2COCl$ or C_6H_5COCl, $CHCl_3$, r.t.; (c) trifluoroacetic acid, CH_2Cl_2.

porphyrin center to produce tetraaldehyde-substituted zinc porphyrin monomer **1**, which was subsequently used as a monomer for the synthesis of porphyrin nanorings. By utilizing 2,4,6-tris(pyridyl-4-yl)-1,3,5-triazine (TPT, **2**) as a template, **1** was mixed with 2,2′-oxydiethanamine (**3**) to perform the aldehyde-amine condensation reaction, during which the coordination of porphyrin central metal with the pyridyl groups on TPT acts as the template to generate a TPT-coordinated triporphyrin nanoring (**4**). The proton nuclear magnetic resonance (^{1}H NMR) spectrum of the crude reaction mixture showed only one set of main peaks that could be attributed to the nanoring **4** (Fig. 1), indicating high efficiency of the self-assembly process. This triporphyrin nanoring has a triangular prism shape, in which three adjacent porphyrin units are linked to each other by six molecules of **3** through the dynamically reversible imine bonds. Due to the instability of imine bonds, the porphyrin nanoring **4** is not very stable after removal of the reaction solvents. Therefore, we further reduced the imine bonds using a mild reducing agent, sodium borohydride acetate, to obtain the reduced triporphyrin nanoring **5** in which the porphyrin units were connected by stable C–N single bonds. Furthermore, *n*-butyryl or benzoyl groups were

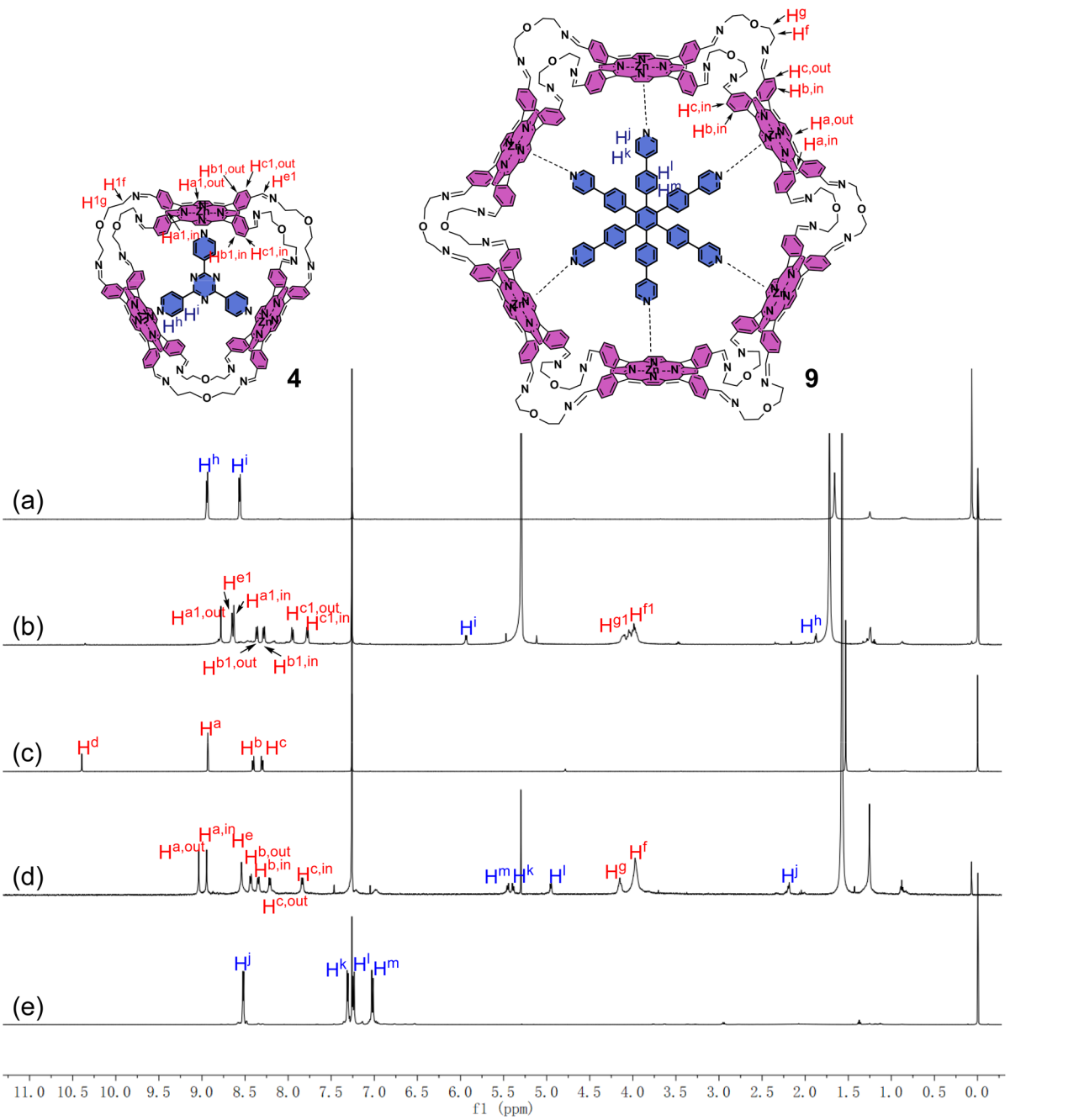

Fig. 1 ^{1}H NMR spectra (500 MHz, $CDCl_3$, 25 °C) of (a) the template **2**, (b) the reaction mixture for synthesis of **4**, (c) monomer **1**, (d) the reaction mixture for synthesis of **9**, and (e) the template **8**.

introduced through an amidation reaction to increase the stability and solubility of the nanoring. Stable and well soluble triporphyrin nanorings **6a** and **6b** were generated in an overall yield of 36% and 46%, respectively, after three-step sequential reactions from the monomer **1** and purification by recrystallization. After removal of the TPT template and zinc ions from **6a** using trifluoroacetic acid, the empty triporphyrin nanoring **7a** with a three-dimensional cylindrical cavity was acquired in 88% yield.

Synthesis of hexaporphyrin nanorings

Afterwards, this strategy was extended to a hexaporphyrin system. Hexaporphyrin nanoring **9** was synthesized from the porphyrin monomer **1** by the formation of imine bonds with **3** in the presence of the hexadentate template **8**, in which a total of 24 aldehyde groups from 6 porphyrin monomers reacted with 24 amino groups from 12 diamine molecules in one pot to form 24 imine bonds. Similarly, almost only one set of peaks was found in the ^{1}H NMR spectrum of the crude reaction mixture (Fig. 1), indicative of high efficiency of the transformation. Due to the relative instability of imine bonds, the imine nanoring **9** was also reduced by sodium borohydride acetate to form **10**, and further underwent the amidation reaction with *n*-butyryl chloride or benzoyl chloride to obtain the stable hexaporphyrin nanorings **11a** and **11b** in a total yield of 38% and 39%, respectively, starting from **1**. Subsequently, under the action of trifluoroacetic acid, the hexapyridine template and zinc ions in **11a** were removed to produce the vacant nanoring **12a** in 84% yield.

Characterization of triporphyrin and hexaporphyrin nanorings

The formation of the coordination complexes and imine nanorings was first characterized by ^{1}H NMR spectroscopy. When the Zn-porphyrin **1** coordinated with the template ligand **2**, the signals of aldehyde hydrogens H^d, pyrrole hydrogens H^a and phenylene hydrogens (H^b and H^c) of **1**, as well as the pyridyl protons H^h and H^i of the template **2** all shifted upfield, indicating the formation of coordination self-assembly (Fig. S3†). After addition of the amine component **3**, the peak of aldehyde hydrogen (H^d) at a chemical shift of 10.39 ppm disappeared, while an imine characteristic peak (H^{e1}) appeared at a chemical shift of around 8.65 ppm (Fig. 1). Simultaneously, the signals of pyrrole hydrogens (H^a) and phenylene hydrogens (H^b and H^c) on the porphyrin shifted upfield, and both split from one set of peaks to two sets of peaks. This is attributed to the asymmetric structure and restrictions on rapid exchange of the porphyrin units after the formation of nanoring **4**, while coordination of the porphyrin monomers with the template can undergo rapid ligand exchange. In the nanoring structure, pyrrole hydrogens and phenylene hydrogens exist in two different chemical environments, towards the inside and outside of the cavity, respectively. The porphyrin nanoring has a relatively strong shielding effect on hydrogens pointing towards the inside, causing the same group of hydrogens to split into two sets of peaks with significant chemical shift differences. Additionally, owing to the highly strong shielding effect, the two peaks corresponding to the pyridyl protons (H^h and H^i) on the template **2** shifted significantly towards the high field (Fig. 1 and S3†). These observations provided solid evidence for the formation of imine triporphyrin nanoring **4**. After reduction of **4** using sodium borohydride acetate, the chemical shifts of almost all hydrogens changed. More importantly, the imine peak with a chemical shift of around 8.65 ppm disappeared and was accompanied by the appearance of a new set of methylene peaks at around 4.0 ppm, indicating the complete reduction of all 12 imine bonds on the porphyrin nanoring and confirming the formation of the reduced triporphyrin nanoring **5** (Fig. S4†).

Similarly, in the case of the hexaporphyrin system, the aldehyde hydrogen peak at a chemical shift of 10.39 ppm disappeared and an imine characteristic peak appeared at a chemical shift of 8.54 ppm after the addition of **3** (Fig. 1 and S15†). The pyrrole protons (H^a) and phenylene protons (H^b and H^c) on the porphyrin units shifted downfield or upfield and split from the original set of peaks into two sets. Meanwhile, the signals of hydrogens (H^j, H^k, H^l and H^m) on the template **8** shifted upfield remarkably (Fig. 1 and S15†) due to the strong shielding effect after the formation of the nanoring. All of these indicated the fabrication of hexaporphyrin nanoring **9**. After reduction with sodium borohydride acetate and then acylation with *n*-butyryl chloride or benzoyl chloride, the appearance of *n*-butyryl or benzoyl peaks and changes in the other ^{1}H NMR signals confirmed the generation of hexaporphyrin nanorings **11a** (Fig. S16†) and **11b** (Fig. S20†).

The structures of the stable nanorings were further confirmed by ^{13}C NMR, ^{1}H–^{1}H correlation spectroscopy (^{1}H–^{1}H COSY), and heteronuclear single-quantum coherence (HSQC). In the ^{1}H–^{1}H COSY spectra of **6a** (Fig. S7†), **6b** (Fig. S11†), **11a** (Fig. S18†) and **11b** (Fig. S22†), correlations were found between $H^{b,\,in}$ and $H^{c,\,in}$ as well as $H^{b,\,out}$ and $H^{c,\,out}$. In the ^{1}H–^{1}H COSY spectra of **6a** (Fig. S7†) and **6b** (Fig. S11†), correlations between H^h and H^i were observed, confirming the existence of template **2** in the triporphyrin nanorings **6a** and **6b**. Similarly, in the ^{1}H–^{1}H COSY spectra of **11a** (Fig. S18†) and **11b** (Fig. S22†), there were correlations between H^j and H^k as well as H^l and H^m, confirming the existence of template **8** in the hexaporphyrin nanorings **11a** and **11b**.

Matrix-assisted laser desorption/ionization time-of-flight mass spectrometry (MALDI-TOF MS) was performed to further confirm the formation of the nanorings. The peaks attributed to $[M - \mathbf{2} + H]^+$ were found at $m/z = 3644.261$ (Fig. 2a and S26†) for **6a**, and at $m/z = 4053.328$ (Fig. S27†) for **6b**, respectively. For **7a**, there was a related peak found at $m/z = 3455.323$ (Fig. 2b and S28†), corresponding to $[M + H]^+$. Relevant peaks attributed to $[M - \mathbf{8} + H]^+$ were observed at $m/z = 7288.965$ (Fig. 2c and S29†) and $m/z = 8104.649$ (Fig S30†) for **11a** and **11b**, respectively. A high peak at $m/z = 6909.277$ (Fig. 2d and S31†) was found for **12a**, attributed to $[M + H]^+$. These peaks are very close to their theoretical simulation values, and the distributions of all isotope peaks are uniform and also well matched with their theoretical calculation values.

In spite of the high flexibility of the 2,2′-oxydiethanamine linker units, we fortunately obtained X-ray quality single crystals

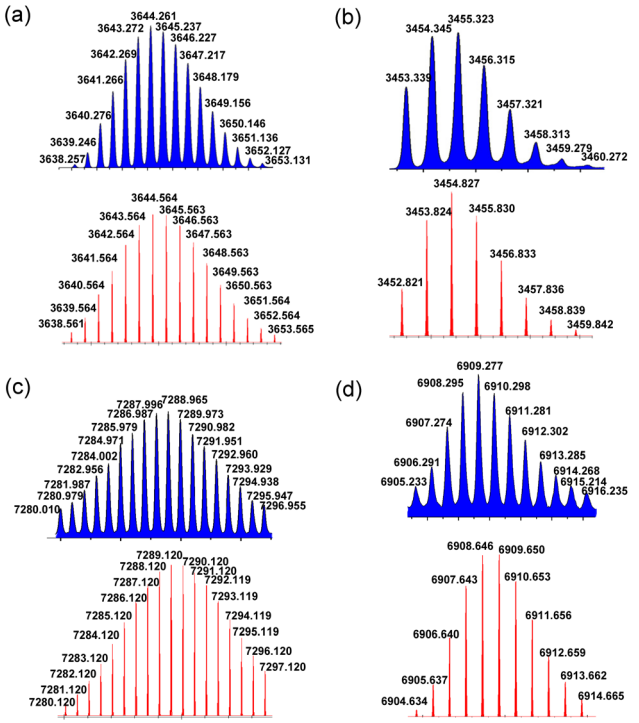

Fig. 2 Experimental (blue) and calculated (red) MALDI-TOF MS spectra (positive reflection mode) of (a) [**6a** − **2** + H]$^+$, (b) [**7a** + H]$^+$, (c) [**11a** − **8** + H]$^+$, and (d) [**12a** + H]$^+$.

of the benzoyl-substituted triporphyrin nanoring **6b** by vapor diffusion of acetone into a chloroform solution of **6b**. The single crystal X-ray analysis unambiguously confirmed the generation of triporphyrin nanorings (Fig. 3). The solid-state structure of **6b** revealed that the triporphyrin nanoring has a symmetrical triangular prism geometry, in which three zinc porphyrins are located on the periphery of the prism and are bridged each other by six 2,2′-oxydiethanamine units. One TPT template axially coordinates with the three zinc porphyrins inside the prism, which further stabilizes the whole structure of the nanoring, while twelve benzoyl groups point outward from the edges of the prism.

Host–guest complexation of porphyrin nanorings and fullerenes

The large cavities of the prepared empty porphyrin nanorings and the donor–acceptor interaction between porphyrins and fullerene guests make them an excellent class of fullerene inclusion hosts. The host–guest complexation of the porphyrin nanorings **7a** and **12a** with fullerenes was systemically studied through UV-vis absorption spectroscopy and fluorescence spectroscopy. The UV-vis and fluorescence spectra (Fig. 4) of triporphyrin nanoring **7a**, C_{60}@**7a**, and C_{70}@**7a** in chloroform were recorded, respectively. Due to the π–π* transition of porphyrins, **7a** has a clear specific absorption peak at 417 nm. Encapsulation of fullerenes caused a red shift phenomenon. The complexation of fullerenes can also be confirmed by the changes in fluorescence spectra. Under the excitation of light at $\lambda = 417$ nm, the nanoring **7a** exhibited significant fluorescence

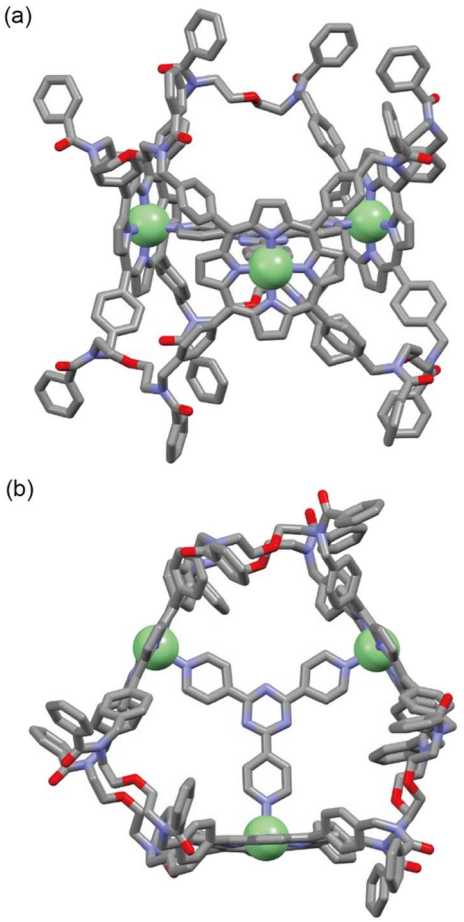

Fig. 3 Single crystal structure of **6b** from side view (a) and top view (b). The solvents, counterions and H atoms have been omitted for clarity. Color code: gray = C; red = O; blue = N; green = Zn^{2+}.

at $\lambda = 654$ nm. Due to the strong host–guest interaction between the nanoring and fullerenes, obvious fluorescence quenching was observed after the addition of fullerene guests.

The host–guest complexation between **7a** and fullerenes was further confirmed by NMR spectroscopy and mass spectrometry. The comparison of ^{1}H NMR spectra (Fig. 5) showed

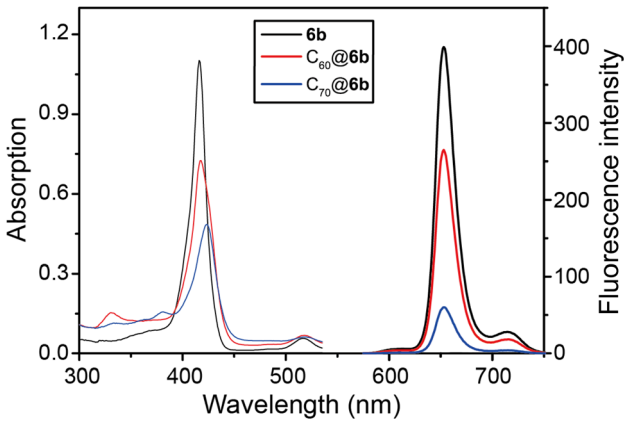

Fig. 4 UV-vis (left) and fluorescence (right) ($\lambda_{ex} = 417$ nm, chloroform, 1×10^{-6} M, room temperature) spectra of **7a**, C_{60}@**7a**, and C_{70}@**7a**.

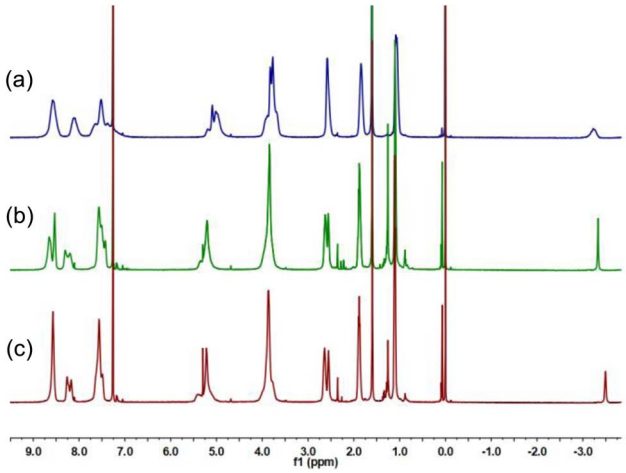

Fig. 5 ^{1}H NMR spectra (500 MHz, $CDCl_3$, 25 °C) of (a) **7a**, (b) C_{60}@**7a**, and (c) C_{70}@**7a**.

significant changes in the chemical shifts of hydrogens on **7a** after it was transformed to C_{60}@**7a** and C_{70}@**7a**. These changes in chemical shifts are attributed to the host–guest complexation and donor–acceptor interactions. The ESI-MS spectrum of **7a** showed a related peak at m/z = 1749.909 (Fig. 6a and b), which corresponds to $[\mathbf{7a} + 2Na]^{2+}$. Comparatively, a peak at m/z = 2110.893 was observed in the ESI-MS spectrum of C_{60}@**7a** (Fig. 6a and c), corresponding to $[C_{60}@\mathbf{7a} + 2Na]^{2+}$. Similarly,

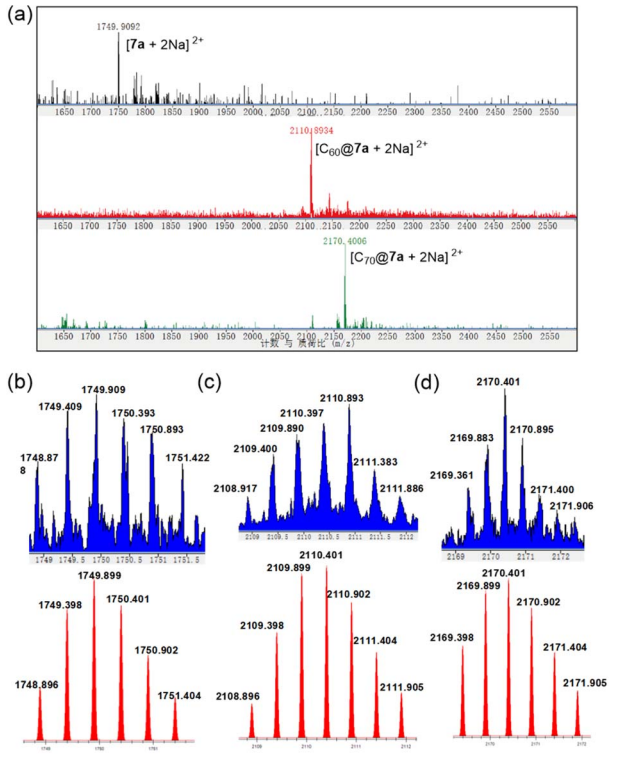

Fig. 6 ESI-MS spectra of the host–guest complex formation. (a) 2^+ charge fragment of **7a** (black), C_{60}@**7a** (red), and C_{70}@**7a** (green). Isotopic distribution spectra (blue) and simulated spectra (red) of (b) **7a**, (c) C_{60}@**7a**, and (d) C_{70}@**7a**.

there was a peak at m/z = 2170.401 found in the ESI-MS spectrum of C_{70}@**7a** (Fig. 6a and d), corresponding to $[C_{70}@\mathbf{7a} + 2Na]^{2+}$. These peaks are in good agreement with their theoretical calculation values and no peaks are found for the complexes with other stoichiometries, suggesting the formation of 1 : 1 host–guest complexes C_{60}@**7a** and C_{70}@**7a**.

The 1 : 1 binding stoichiometric ratio between the nanoring **7a** or **12a** and C_{60} or C_{70} was further confirmed by using the Job plot experiments based on UV-vis spectroscopy (Fig. S32, S33, S34 and S35†). The binding affinities were then determined with the titration method based on fluorescence spectroscopy. The association constants (K_a) of C_{60}@**7a** and C_{70}@**7a** in toluene were measured to be 5.56 (±0.04) × 10^5 M^{-1} and 5.94 (±0.12) × 10^6 M^{-1}, respectively (Fig. S36 and S37†), while the K_a of C_{60}@**12a** and C_{70}@**12a** in dichloromethane/toluene (95/5) was 4.14 (±0.03) × 10^4 M^{-1} and 2.84 (±0.02) × 10^5 M^{-1}, respectively (Fig. S38 and S39†). These data indicate that the triporphyrin and hexaporphyrin nanorings have comparable binding ability towards C_{60} and C_{70} compared with the other cyclic porphyrin-based receptors.[14a,15b,16d,18] The relative weaker binding ability of **12a** with C_{60} and C_{70} than that of **7a** is probably because the cavity of **12a** is too large for C_{60} and C_{70}. Similar to some previously reported porphyrin-based receptors for fullerenes,[14a,18] it can also be found that the K_a of C_{70}@**7a** is one order of magnitude higher than that of C_{60}@**7a**, and K_a of C_{70}@**12a** is also almost one order of magnitude higher than that of C_{60}@**12a**. The higher binding capability for C_{70} can also be reflected in UV-vis and fluorescence spectroscopy. By comparison with encapsulation of C_{60}, encapsulation of C_{70} induces a more significant red shift and the fluorescence quenching of C_{70}@**7a** is more pronounced than that of C_{60}@**7a** (Fig. 4), implying the stronger charge transfer interaction between **7a** and C_{70}. All of these indicate that the two nanorings exhibit higher selectivity for C_{70} than for C_{60}. Competitive encapsulation of C_{60}/C_{70} was further studied and the results are provided in the ESI† to reveal the promising applications of these porphyrin nanorings in selective adsorption and separation of C_{70}.

Conclusions

In summary, covalent porphyrin nanorings linked by imine bonds were efficiently prepared by using a template-directed approach through aldehyde-amine condensation reactions. A rigid tripyridine or hexapyridine template was used to coordinate with a tetraaldehyde-derived zinc porphyrin monomer in a molar ratio of 1 : 3 or 1 : 6, and then reacted with a carefully selected diamine molecule to produce a triporphyrin nanoring and a hexaporphyrin nanoring, respectively. Under the action of the template, up to 18 precursor molecules react with each other to generate a nanoring molecule in one step. The imine-linked nanorings are further modified by reduction and acylation reactions to obtain more stable porphyrin nanorings. Their structures were well characterized by ^{1}H, ^{13}C, ^{1}H–^{1}H COSY and HSQC NMR, MALDI-TOF MS spectrometry, as well as single crystal X-ray analysis. The host–guest complexation of *n*-butyryl-derived triporphyrin and hexaporphyrin nanorings with fullerenes C_{60} and C_{70} was investigated using UV-vis and fluorescence

spectroscopy. It was found that they could effectively encapsulate C_{60} and C_{70} in a 1 : 1 binding stoichiometry, with a complexation constant of 4.14 ($\pm$0.03) $\times$ 10^4 $\sim$ 5.94 ($\pm$0.12) $\times$ 10^6 M^{-1}. In comparison with the encapsulation of C_{60}, the triporphyrin nanorings have an apparently higher binding affinity towards C_{70}. The presented work provides a new insight into highly efficient construction of three-dimensional porphyrin cages and their applications in host–guest recognition.

Data availability

Data supporting this article have been included in the ESI.†

Author contributions

Conceptualization: S. Li; data curation and methodology: Z. Xu, J. Liu, M. Little, Y. Xie, Z. Zhang, and L. Yu; synthesis, host–guest complexation and analysis: Z. Xu, W. Ying, Y. Li, X. Dong, J. Liu, S. Wang, and D. Zhang; writing – original draft: Z. Xu; writing – review & editing: S. Wang, F. Huang, and S. Li.

Conflicts of interest

There are no conflicts to declare.

Acknowledgements

We thank Professor Andrew I. Cooper (Department of Chemistry and Materials Innovation Factory, University of Liverpool, Liverpool L7 3NY, U.K.) for his advice on the self-assembly of porphyrin nanorings. S.L. thanks the National Natural Science Foundation of China (22071040) and the Natural Science Foundation of Zhejiang Province (LZ24B020005) for financial support. F.H. thanks the National Key Research and Development Program of China (2021YFA0910100), the National Natural Science Foundation of China (22035006, 22320102001, and 22350007), the Zhejiang Provincial Natural Science Foundation of China (LD21B020001), the Starry Night Science Fund of Zhejiang University Shanghai Institute for Advanced Study (SN-ZJU-SIAS-006), and the Leading Innovation Team grant from the Department of Science and Technology of Zhejiang Province (2022R01005) for financial support.

Notes and references

1 (*a*) S. R. Seidel and P. J. Stang, *Acc. Chem. Res.*, 2002, **35**, 972–983; (*b*) M. Yoshizawa and M. Fujita, *Angew. Chem., Int. Ed.*, 2009, **48**, 3418–3438; (*c*) T. R. Cook and P. J. Stang, *Chem. Rev.*, 2013, **113**, 734–777; (*d*) C. T. McTernan and J. R. Nitschke, *Chem. Rev.*, 2022, **122**, 10393–10437; (*e*) X. Yang and C. T. Yavuz, *Chem. Rev.*, 2023, **123**, 4602–4634; (*f*) R. Ham, C. J. Nielsen, S. Pullen and J. N. H Reek, *Chem. Rev.*, 2023, **123**, 5225–5261.

2 (*a*) Z. Lu, T. K. Ronson, A. W. Heard, S. Feldmann, N. Vanthuyne, A. Martinez and J. R. Nitschke, *Nat. Chem.*, 2023, **15**, 405–412; (*b*) A. He, Z. Jiang, Y. Wu, H. Hussain, J. Rawle, M. E. Briggs, M. A. Little, A. G. Livingston and A. I. Cooper, *Nat. Mater.*, 2022, **21**, 463–470; (*c*) A. Kewley, A. Stephenson, L. Chen, M. E. Briggs, T. Hasell and A. I. Cooper, *Chem. Mater.*, 2015, **27**, 3207–3210; (*d*) Y. Zhang, Y. Jiao, X. Jia, Q. Guo and C. Duan, *Chin. Chem. Lett.*, 2024, **35**, 108748; (*e*) A. Kewley, A. Stephenson, L. Chen, M. E. Briggs, T. Hasell and A. I. Cooper, *Nat. Rev. Chem*, 2021, **5**, 168–182.

3 (*a*) L. Chen, P. S. Reiss, S. Y. Chong, D. Holden, K. E. Jelfs, T. Hasell, M. A. Little, A. Kewley, M. E. Briggs, A. Stephenson, K. M. Thomas, J. A. Armstrong, J. Bell, J. Busto, R. Noel, J. Liu, D. M. Strachan, P. K. Thallapally and A. I. Cooper, *Nat. Mater.*, 2014, **13**, 954–960; (*b*) C. Zhu, K. Yang, H. Wang, Y. Fang, L. Feng, J. Zhang, Z. Xiao, X. Wu, Y. Li, Y. Fu, W. Zhang, K.-Y. Wang and H.-C. Zhou, *ACS Cent. Sci.*, 2022, **8**, 562–570; (*c*) P. Bhandari and P. S. Mukherjee, *ACS Catal.*, 2023, **13**, 6126–6143.

4 (*a*) X. Li, W. Lin, V. Sharma, R. Gorecki, M. Ghosh, B. A. Moosa, S. Aristizabal, S. Hong, N. M. Khashab and S. P. Nunes, *Nat. Commun.*, 2023, **14**, 3112; (*b*) Y. Fang, J. A. Powell, E. Li, Q. Wang, Z. Perry, A. Kirchon, X. Yang, Z. Xiao, C. Zhu, L. Zhang, F. Huang and H.-C. Zhou, *Chem. Soc. Rev.*, 2019, **48**, 4707–4730; (*c*) M. R. Crawley, D. Zhang, A. N. Oldacre, C. M. Beavers, A. E. Friedman and T. R. Cook, *J. Am. Chem. Soc.*, 2021, **143**, 1098–1106; (*d*) M. Hua, S. Wang, Y. Gong, J. Wei, Z. Yang and J.-K. Sun, *Angew. Chem., Int. Ed.*, 2021, **60**, 12490–12497.

5 (*a*) M. Mastalerz, M. W. Schneider, I. M. Oppel and O. Presly, *Angew. Chem., Int. Ed.*, 2011, **50**, 1046–1051; (*b*) M. Liu, L. Zhang, M. A. Little, V. Kapil, M. Ceriotti, S. Yang, L. Ding, D. L. Holden, R. Balderas-Xicohténcatl, D. He, R. Clowes, S. Y. Chong, G. Schütz, L. Chen, M. Hirscher and A. I. Cooper, *Science*, 2019, **366**, 613–620; (*c*) W. Zhou, A. Li, M. Zhou, Y. Xu, Y. Zhang and Q. He, *Nat. Commun.*, 2023, **14**, 5388; (*d*) G. Zhang, B. Hua, A. Dey, M. Ghosh, B. A. Moosa and N. M. Khashab, *Acc. Chem. Res.*, 2021, **54**, 155–168; (*e*) C. Liu, W. Li, Y. Liu, H. Wang, B. Yu, Z. Bao and J. Jiang, *Chem. Eng. J.*, 2022, **428**, 131129; (*f*) W. Wang, K. Su and D. Yuan, *Mater. Chem. Front.*, 2023, **7**, 5247–5262.

6 J. Li, P. Nowak and S. Otto, *J. Am. Chem. Soc.*, 2013, **135**, 9222–9239.

7 G. Montà-González, F. Sancenón, R. Martínez-Máñez and V. Martí-Centelles, *Chem. Rev.*, 2022, **122**, 13636–13708.

8 (*a*) S. J. Rowan, S. J. Cantrill, G. R. L. Cousins, J. K. M. Sanders and J. F. Stoddart, *Angew. Chem., Int. Ed.*, 2002, **41**, 898–952; (*b*) P. T. Corbett, J. Leclaire, L. Vial, K. R. West, J. L. Wietor, J. K. M. Sanders and S. Otto, *Chem. Rev.*, 2006, **106**, 3652–3711; (*c*) Z. Shan, X. Wu, B. Xu, Y.-L. Hong, M. Wu, Y. Wang, Y. Nishiyama, J. Zhu, S. Horike, S. Kitagawa and G. Zhang, *J. Am. Chem. Soc.*, 2020, **142**, 21279–21284; (*d*) F. B. L. Cougnon, A. R. Stefankiewicz and S. Ulrich, *Chem. Sci.*, 2024, **15**, 879–895.

9 (*a*) S. Klotzbach and F. Beuerle, *Angew. Chem., Int. Ed.*, 2015, **54**, 10356–10360; (*b*) M. Mastalerz, *Acc. Chem. Res.*, 2018, **51**, 2411–2422; (*c*) K. Acharyya and P. S. Mukherjee, *Angew. Chem., Int. Ed.*, 2019, **58**, 8640–8653; (*d*) M. A. Little and A. I. Cooper, *Adv. Funct. Mater.*, 2020, 1909842; (*e*) C. F. M. Mirabella, G. Aragay and P. Ballester, *Chem. Sci.*, 2023, **14**, 186–195.

10 (*a*) C. D. Meyer, C. S. Joiner and J. F. Stoddart, *Chem. Soc. Rev.*, 2007, **36**, 1705–1723; (*b*) M. E. Belowich and J. F. Stoddart, *Chem. Soc. Rev.*, 2012, **41**, 2003–2024.

11 Y. Jin, C. Yu, R. J. Denman and W. Zhang, *Chem. Soc. Rev.*, 2013, **42**, 6634–6654.

12 (*a*) Z. Wang, Q.-P. Zhang, F. Guo, H. Ma, Z.-H. Liang, C.-H. Yi, C. Zhang and C.-F. Chen, *Nat. Commun.*, 2024, **15**, 670; (*b*) Y. Lei, Z. Li, G. Wu, L. Zhang, L. Tong, T. Tong, Q. Chen, L. Wang, C. Ge, Y. Wei, Y. Pan, A. C.-H. Sue, L. Wang, F. Huang and H. Li, *Nat. Commun.*, 2022, **13**, 3557; (*c*) T. Kunde, E. Nieland, H. V. Schroder, C. A. Schalley and B. M. Schmidt, *Chem. Commun.*, 2020, **56**, 4761–4764; (*d*) E. Ramakrishna, J. D. Tang, J. J. Tao, Q. Fang, Z. B. Zhang, J. Y. Huang and S. J. Li, *Chem. Commun.*, 2021, **57**, 9088–9091; (*e*) H. H. Huang, K. S. Song, A. Prescimone, A. Aster, G. Cohen, R. Mannancherry, E. Vauthey, A. Coskun and T. Solomek, *Chem. Sci.*, 2021, **12**, 5275–5285; (*f*) X. Yu, B. Wang, Y. Kim, J. Park, S. Ghosh, B. Dhara, R. D. Mukhopadhyay, J. Koo, I. Kim, S. Hwang, I.-C. Hwang, S. Seki, D. M. Guldi, M.-H. Baik and K. Kim, *J. Am. Chem. Soc.*, 2020, **142**, 12596–12601.

13 (*a*) J. Koo, I. Kim, Y. Kim, D. Cho, I. Hwang, R. D. Mukhopadhyay, H. Song, Y. H. Ko, A. Dhamija, H. Lee, W. Hwang, S. Kim, M. Baik and K. Kim, *Chem*, 2020, **6**, 3374–3384; (*b*) C. Liu, K. Liu, C. Wang, H. Liu, H. Wang, H. Su, X. Li, B. Chen and J. Jiang, *Nat. Commun.*, 2020, **11**, 1047; (*c*) T. Jiao, H. Qu, L. Tong, X. Cao and H. Li, *Angew. Chem., Int. Ed.*, 2021, **60**, 9852–9858; (*d*) B. P. Benke, T. Kirschbaum, J. Graf, J. H Gross and M. Mastalerz, *Nat. Chem.*, 2023, **15**, 413–423.

14 (*a*) C. Zhang, Q. Wang, H. Long and W. Zhang, *J. Am. Chem. Soc.*, 2011, **133**, 20995–21001; (*b*) F. Hajjaj, K. Tashiro, H. Nikawa, N. Mizorogi, T. Akasaka, S. Nagase, K. Furukawa, T. Kato and T. Aida, *J. Am. Chem. Soc.*, 2011, **133**, 9290–9292; (*c*) J. Zhang, Y. Li, W. Yang, S. Lai, C. Zhou, H. Liu, C. Che and Y. Li, *Chem. Commun.*, 2012, **48**, 3602–3604; (*d*) A. Ouchi, K. Tashiro, K. Yamaguchi, T. Tsuchiya, T. Akasaka and T. Aida, *Angew. Chem., Int. Ed.*, 2006, **45**, 3542–3546; (*e*) H. Wang, Y. Jin, N. Sun, W. Zhang and J. Jiang, *Chem. Soc. Rev.*, 2021, **50**, 8874–8886; (*f*) Y. Ding, J. Wang, R. Wang and Y. Xie, *Chin. Chem. Lett.*, 2024, **35**, 109008; (*g*) B. Bishop, S. Huang, H. Chen, H. Yu, H. Long, J. Shen and W. Zhang, *Chin. Chem. Lett.*, 2024, **35**, 109966; (*h*) F. Wang, C. Bucher, Q. He, A. Jana and J. L. Sessler, *Acc. Chem. Res.*, 2022, **55**, 1646–1658; (*i*) Y. Wang, X.-S. Ke, S. Lee, S. Kang, V. M. Lynch, D. Kim and J. L. Sessler, *J. Am. Chem. Soc.*, 2022, **144**, 9212–9216; (*j*) J. Dong, Y. Wang, Y.-L. Lu and L. Zhang, *Chin. Chem. Lett.*, 2023, **34**, 108052.

15 (*a*) S. Durot, J. Taesch and V. Heitz, *Chem. Rev.*, 2014, **114**, 8542–8578; (*b*) J. Song, N. Aratani, H. Shinokubo and A. Osuka, *J. Am. Chem. Soc.*, 2010, **132**, 16356–16357; (*c*) C. Maeda, S. Toyama, N. Okada, K. Takaishi, S. Kang, D. Kim and T. Ema, *J. Am. Chem. Soc.*, 2020, **142**, 15661–15666; (*d*) R. D. Mukhopadhyay, Y. Kim, J. Koo and K. Kim, *Acc. Chem. Res.*, 2018, **51**, 2730–2738; (*e*) S. Liu, D. V. Kondratuk, S. A. L. Rousseaux, G. Gil-Ramírez, M. C. O'Sullivan, J. Cremers, T. D. W. Claridge and H. L. Anderson, *Angew. Chem., Int. Ed.*, 2015, **54**, 5355–5359; (*f*) P. Liu, Y. Hisamune, M. D. Peeks, B. Odell, J. Q. Gong, L. M. Herz and H. L. Anderson, *Angew. Chem., Int. Ed.*, 2016, **55**, 8358–8362; (*g*) X.-S. Ke, T. Kim, Q. He, V. M. Lynch, D. Kim and J. L. Sessler, *J. Am. Chem. Soc.*, 2018, **140**, 16455–16459; (*h*) I. N. Meshkov, V. Bulach, Y. G. Gorbunova, A. Jouaiti, A. A. Sinelshchikova, N. Kyritsakas, M. S. Grigoriev, A. Y. Tsivadze and M. W. Hosseini, *New J. Chem.*, 2018, **42**, 7816–7822; (*i*) J. Liu, H. Chen, Y. Lv, H. Wu, L. Yang, J. Zhang, J. Huang and W. Wang, *J. Agric. Food Chem.*, 2024, **72**, 11185–11194; (*j*) H. Chen, I. Roy, M. S. Myong, J. S. W. Seale, K. Cai, Y. Jiao, W. Liu, B. Song, L. Zhang, X. Zhao, Y. Feng, F. Liu, R. M. Young, M. R. Wasielewski and J. F. Stoddart, *J. Am. Chem. Soc.*, 2023, **145**, 10061–10070; (*k*) V. Iannace, C. Sabrià, Y. Xu, M. von Delius, I. Imaz, D. Maspoch, F. Feixas and X. Ribas, *J. Am. Chem. Soc.*, 2024, **146**, 5186–5194.

16 (*a*) J. K. Sprafke, D. V. Kondratuk, M. Wykes, A. L. Thompson, M. Hoffmann, R. Drevinskas, W.-H. Chen, C. K. Yong, J. Kärnbratt, J. E. Bullock, M. Malfois, M. R. Wasielewski, B. Albinsson, L. M. Herz, D. Zigmantas, D. Beljonne and H. L. Anderson, *J. Am. Chem. Soc.*, 2011, **133**, 17262–17273; (*b*) M. C. O'Sullivan, J. K. Sprafke, D. V. Kondratuk, C. Rinfray, T. D. W. Claridge, A. Saywell, M. O. Blunt, J. N. O'Shea, P. H. Beton, M. Malfois and H. L. Anderson, *Nature*, 2011, **469**, 72–75; (*c*) B. Zhu, H. Chen, W. Lin, Y. Ye, J. Wu and S. Li, *J. Am. Chem. Soc.*, 2014, **136**, 15126–15129; (*d*) S. Wang, Y. Shen, B. Zhu, J. Wu and S. Li, *Chem. Commun.*, 2016, **52**, 10205–10216; (*e*) P. S. Bols and H. L. Anderson, *Acc. Chem. Res.*, 2018, **51**, 2083–2092; (*f*) J. M. Van Raden, J.-R. Deng, H. Gotfredsen, J. Hergenhahn, M. Clarke, M. Edmondson, J. Hart, J. N. O'Shea, F. Duarte, A. Saywell and H. L. Anderson, *Angew. Chem., Int. Ed.*, 2024, **63**, e202400103; (*g*) R. Haver, L. Tejerina, H.-W. Jiang, M. Rickhaus, M. Jirasek, I. Grübner, H. J. Eggimann, L. M. Herz and H. L. Anderson, *J. Am. Chem. Soc.*, 2019, **141**, 7965–7971; (*h*) M. A. Majewski, W. Stawski, J. M. Van Raden, M. Clarke, J. Hart, J. N. O'Shea, A. Saywell and H. L. Anderson, *Angew. Chem., Int. Ed.*, 2023, **62**, e202302114.

17 (*a*) H. L. Anderson and J. K. M. Sanders, *Angew. Chem., Int. Ed.*, 1990, **29**, 1400–1403; (*b*) M. Hoffmann and H. L. Anderson, *Angew. Chem., Int. Ed.*, 2008, **47**, 4993–4996.

18 (*a*) Y. Shi, K. Cai, H. Xiao, Z. Liu, J. Zhou, D. Shen, Y. Qiu, Q. H. Guo, C. Stern, M. R. Wasielewski, F. Diederich, W. A. Goddard III and J. F. Stoddart, *J. Am. Chem. Soc.*, 2018, **140**, 13835–13842; (*b*) P. Mondal and S. P. Rath, *Chem.–Asian J.*, 2017, **12**, 1824–1835; (*c*) J. Pfeuffer-Rooschüz, S. Heim, A. Prescimone and K. Tiefenbacher, *Angew. Chem., Int. Ed.*, 2022, **61**, e202209885; (*d*) H. Nian, S.-M. Wang, Y.-F. Wang, Y.-T. Zheng, L.-S. Zheng, X. Wang, L.-P. Yang, W. Jiang and L. Cao, *Chem. Sci.*, 2024, **15**, 10214–10220; (*e*) Q. Chen, A. L. Thompson, K. E. Christensen, P. N. Horton, S. J. Coles and H. L. Anderson, *J. Am. Chem. Soc.*, 2023, **145**, 11859–11865.